Research

Author for correspondence:
Anton Zilman
e-mail: zilmana@physics.utoronto.ca

THE ROYAL SOCIETY PUBLISHING

Effects of niche overlap on coexistence, fixation and invasion in a population of two interacting species

Matthew Badali[1] and Anton Zilman[1,2]

[1]Department of Physics, University of Toronto, 60 St George St., Toronto, Canada M5S 1A7
[2]Institute for Biomaterials and Biomedical Engineering, University of Toronto, Toronto, Canada

MB, 0000-0002-1198-2770

Synergistic and antagonistic interactions in multi-species populations—such as resource sharing and competition—result in remarkably diverse behaviours in populations of interacting cells, such as in soil or human microbiomes, or clonal competition in cancer. The degree of inter- and intra-specific interaction can often be quantified through the notion of an ecological 'niche'. Typically, weakly interacting species that occupy largely distinct niches result in stable mixed populations, while strong interactions and competition for the same niche result in rapid extinctions of some species and fixations of others. We investigate the transition of a deterministically stable mixed population to a stochasticity-induced fixation as a function of the niche overlap between the two species. We also investigate the effect of the niche overlap on the population stability with respect to external invasions. Our results have important implications for a number of experimental systems.

1. Introduction

Remarkable biodiversity exists in biomes such as the human microbiome [1–3], the ocean surface [4,5], soil [6], the immune system [7–9] and other ecosystems [10,11]. Accordingly, quantitative predictive understanding of the long-term population behaviour of complex populations is important for many human health and disease and industrial processes such as drug resistance in bacteria, cancer progression, evolutionary phylogeny inference algorithms and immune response [2,3,12–17]. Nevertheless, the long-term dynamics, diversity and stability of communities of multiple interacting species are still incompletely understood.

One common theory, known as the Gause's rule or the competitive exclusion principle, postulates that due to abiotic constraints, resource usage, inter-species interactions and other factors, ecosystems can be divided into ecological niches, with each niche supporting only one species in steady state; that species is termed to have fixated within the niche [18–21]. Commonly, the number of ecological niches can be related to the number of limiting factors that affect growth and death rates, such as metabolic resources or secreted molecular signals like growth factors or toxins, or other regulatory molecules [22–25]. The strength of inter-species interactions can be commonly characterized by a quantity known as a niche overlap [26–30]. Observed biodiversity can also arise from the turnover of transient mutants or immigrants that appear and go extinct in the population [31–33]. However, the exact definition of an ecological niche is still a subject of debate and varies among different works [4,27,30,34–38]. The maintenance of the biodiversity of species that occupy similar niches is still not fully understood [25,39,40].

Deterministically, ecological dynamics of mixed populations has been commonly described as a dynamical system of equations that governs the dynamics of the numbers of individuals of each species and the concentrations of the limiting factors [22–24]. Steady-state coexistence of multiple species commonly corresponds to a stable fixed point in such a dynamical system, and the number of stably coexisting species is typically constrained by the number of limiting factors [22–24]. In some cases, deterministic models allow coexistence of more species than the number of limiting factors, for instance, when the attractor of the system dynamics is a limit cycle rather than a fixed point [24,41]. Particularly pertinent for this paper is the case when the interactions of the limiting factors and the target species have a redundancy that results in the transformation of a stable fixed point into a marginally stable manifold of fixed points. This situation underlies many neutral models of population dynamics and evolution [19,20,31,42–45]. However, in this situation, the stochastic fluctuations in the species numbers become important [24,25,46–49].

Stochastic effects, arising either from the extrinsic fluctuations of the environment [50,51], or the intrinsic stochasticity of the individual birth and death events within the population [38,43,52–58], modify the deterministic picture. The latter type of stochasticity, known as demographic noise, is the focus of this paper. Demographic noise causes fluctuations of the populations' abundances around the deterministic steady state until a rare large fluctuation leads to an extinction of one of the species [20,43,57]. In systems with a deterministically stable coexistence point, the mean time to extinction (MTE) is typically exponential in the population size [54,59–62] and is commonly considered to imply stable long-term coexistence for typical biological examples with relatively large numbers of individuals [62,63].

By contrast, in systems with a stable neutral manifold that restore fluctuations out of the manifold but not along it, mean extinction times scale as a power law with the population size, indicating that the coexistence fails in such systems on biologically relevant timescales [42,43,54,64,65]. This type of stochastic dynamics parallels the stochastic fixation in the Moran–Fisher–Wright model that describes strongly competing populations with fixed overall population size, and is the classical example of the class of models known as neutral models [9,14,20,37,42,66–68].

A broad class of dynamical models of multi-species populations interacting through limiting factors can be mapped onto the class of models known as generalized Lotka–Volterra (LV) models, which allow one to conveniently distinguish between various interaction regimes, such as competition or mutualism, and which have served as paradigmatic models for the study of the behaviour of interacting species [30,38,43,46–49,54–58,69,70]. Remarkably, the stochastic dynamics of LV type models is still incompletely understood, and has recently received renewed attention motivated by problems in bacterial ecology and cancer progression [9,25,37,38,57,71–73]. A number of approximations have been used to understand the stochastic dynamics of the LV model, predominantly in the independent regime, or the opposite neutral limit [38,43,54–57,74]. However, the approximations tend to break down for the strong competition near the neutral limit, which is of central importance for understanding the deviations of ecological and physiological systems from neutrality [38,70,75–77].

In this paper, we analyse a LV model of two competing species using the master equation and first passage formalism that enables us to obtain numerically exact solution to arbitrary accuracy in all regimes, avoiding inaccuracies of various approximate descriptions of the stochastic dynamics of the system. The emphasis of this paper is on the effect of the ecological niche overlap on the transition from the deterministic coexistence to the stochastic fixation. In particular, we focus on the balance between the stochastic and deterministic effects in the strong competition regime near-complete niche overlap, as expressed in the interplay between the exponential and algebraic terms in the extinction time as a function of the population size. Furthermore, we study the complementary question of the population stability with respect to the invasion of an immigrant or a mutant into a stable ecological

niche of an already established species. This analysis informs many theories of transient diversity, such as Hubbell's neutral theory, and serves as a stepping stone towards multi-species models in non-neutral regime.

The paper is structured as follows. Section 2 discusses the definition of an ecological niche and briefly examines the regimes of deterministic stability of the system. In §3, we introduce the stochastic description of the LV model. In §3.1, we analyse the fixation/extinction times as a function of the niche overlap between the two species. We find that for any incomplete niche overlap the extinction time contains both terms that scale exponentially and algebraically with the system size, only reaching the known algebraic scaling at complete niche overlap; we calculate the exact functional form of these dependencies. Section 3.2 discusses the dynamic underpinning of the results of §3.1. In §3.3, we consider the invasion of an immigrant or a mutant into a stable ecological niche of an already established species, and calculate the invasion probabilities as a function of the system size and the niche overlap. The probability of success of an invasion attempt depends strongly on the competition strength, decreasing linearly with niche overlap, while only weakly dependent on the system size. All invasion attempts occur rapidly regardless of the outcome, or of the niche overlap between the two species or system size. We conclude with the Discussion section of these results in the context of previous works, and their implications for a number of experimental systems.

2. Deterministic behaviour of the Lotka–Volterra model: overview

The model being employed in this paper is based on the generalized two-dimensional LV equations, that have served as a paradigmatic system to study the behaviour of interacting populations [30,38,43,46–49,54–58,69,70]. An example of the derivation of the model, from the underlying mechanistic model describing the exchange of control factors, is shown in the electronic supplementary material. The dynamical equations of the numbers of individuals of species 1 (denoted as x_1) and species 2 (denoted as x_2) are [57,78,79]

$$\dot{x}_1 = r_1 x_1 \left(1 - \frac{x_1 + a_{12}x_2}{K_1}\right) \quad \text{and} \quad \dot{x}_2 = r_2 x_2 \left(1 - \frac{a_{21}x_1 + x_2}{K_2}\right). \tag{2.1}$$

The turnover rates r_i set the timescales of the birth and death for each species, and K_i are known as the carrying capacities. The interaction parameters a_{ij} provide a mathematical representation of the intuitive notion of the niche overlap between the species, commonly used to characterize the competition of multi-species systems. These niche overlap parameters, which represent the competition between species arising from their shared usage of resources and other factors, dictate the long-term coexistence, viability and the diversity of the population, as well as the apportionment of the different species among different niches [26–30]. The niche overlap parameters can be directly derived from an underlying model describing the production–consumption dynamics of the limiting factors that control the birth and death rates in the system (see electronic supplementary material). When $a_{ij} = 0$, species j does not affect species i, and they occupy separate ecological niches. At the other limit, $a_{ij} = 1$, species j competes just as strongly with species i as species i does within itself, and both species occupy same niche.

The deterministic behaviour of the generalized LV model is well known and can result in various stability regimes, including coexistence, competitive exclusion, mutualism and bi-stability [57,78,79], as reviewed in the electronic supplementary material. Here, we briefly review the behaviour of the deterministic equations (2.1), which have four fixed points [57,78,79]

$$O = (0, 0), \quad A = (0, K_2), \quad B = (K_1, 0) \quad \text{and} \quad C = \left(\frac{K_1 - a_{12}K_2}{1 - a_{12}a_{21}}, \frac{K_2 - a_{21}K_1}{1 - a_{12}a_{21}}\right). \tag{2.2}$$

The origin O is the fixed point corresponding to both species being extinct, and is unstable with positive eigenvalues equal to r_1 and r_2 along the corresponding on-axis eigendirections. The single species fixed points A and B are stable on axis (with eigenvalues $-r_1$ and $-r_2$, respectively), but are unstable with respect to invasion if point C is stable, reflected in the positive second eigenvalue equal to $r_2(1 - a_{21}K_1/K_2)$ and $r_1(1 - a_{12}K_2/K_1)$, respectively. Fixed point C corresponds to the coexistence of the two species and is stable when both $a_{ij} < 1$ for $K_1 = K_2$, also known as the weak competition regime ([57,78,79] and electronic supplementary material).

In the special case $a_{12} = a_{21} = 1$, the stable coexistence point degenerates into a neutral line of stable points, defined by $x_2 = K - x_1$, as shown in figure 1. Each point on the line is stable with respect to
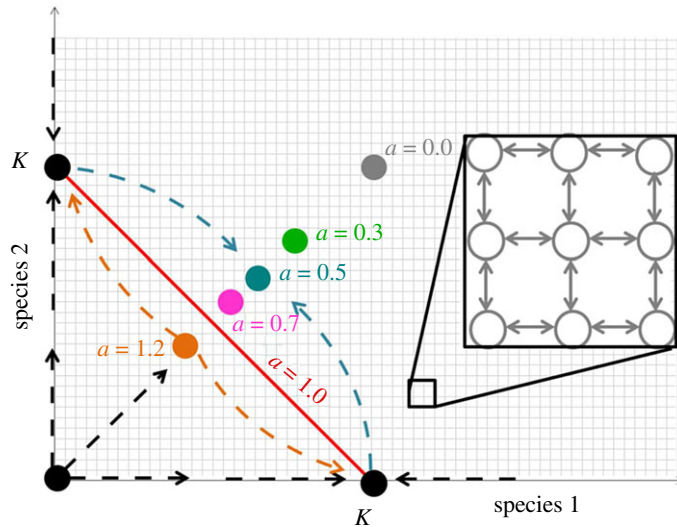
Figure 1. Phase space of the coupled logistic model. Coloured dots show the position of $C = ((K_1 - a_{12} \ K_2)/(1 - a_{12}a_{21}),$ $(K_2 - a_{21} \ K_1)/(1 - a_{12}a_{21}))$ at the indicated values of the niche overlap a for $a_{12} = a_{21} \equiv a$. The fixed point is stable for $a < 1$. At $a = 0$, the two species evolve independently. As a increases, the deterministically stable fixed point moves towards the origin. At $a = 1$, the fixed point degenerates into a line of marginally stable fixed points, corresponding to the Moran model. The dashed lines illustrate the deterministic flow of the system: blue for $a = 0.5$, and orange for $a = 1.2$. The zoom inset illustrates the stochastic transitions between the discrete states of the system. Fixation occurs when the system reaches either of the axes. See text for details.

perturbations off line, but any perturbations along the line are not restored to their unperturbed position [23,80]. This line corresponds to the singular case of complete niche overlap where the two species are functionally identical with respect to their interactions with limiting factors like resources, space, toxins, predators etc. (see also electronic supplementary material). The stochastic dynamics along this line correspond to the classical Moran model [43,56–58] as discussed below, and in the following we refer to this line as the Moran line.

Figure 1 shows the phase portrait of the system, in the symmetric case of $K_1 = K_2 \equiv K$, $r_1 = r_2 \equiv r$ and $a_{12} = a_{21} = a$, where neither of the species has an explicit fitness advantage. This equality of the two species, also known as neutrality, serves as a null model against which systems with explicit fitness differences can be compared.

Stochastic effects, described in the next section, modify the deterministic stability picture and can lead to extinction or fixation of species even in deterministically stable case. In this paper, we focus on the effects of stochasticity in the deterministically stable weak competition regime $(0 \leq a \leq 1)$, finding the scaling of the mean times to fixation and invasion as a function of the niche overlap a and comparing these to the known limits. The results in the asymmetric case are qualitatively similar and are relegated to the electronic supplementary material.

3. Effects of stochasticity

Stochasticity naturally arises in the dynamics of the system from the randomness in the birth and death times of the individuals—commonly known as the demographic noise [52,81–83]. Competitive interactions between the species can affect either the birth rates (such as competition for nutrients) or the death rates (such as toxins or metabolic waste), and in general may result in different stochastic descriptions [84,85]. In this paper, we follow others [43,55,56] in considering the case where the inter-species competition affects the death rates so that the *per capita* birth and death rates b_i and d_i of species i are

$$\frac{b_i}{x_i} = r_i \quad \text{and} \quad \frac{d_i}{x_i} = r_i \frac{x_i + a_{ij}x_j}{K_i}. \tag{3.1}$$

The *per capita* death rate of a member of species i is increased by the presence of other members of the same species, and to a lesser effect (in proportion to their niche overlap) also by members of the other

species. In the deterministic limit of negligible fluctuations, the model recovers the mean field competitive LV equations (2.1) [43]. The effects of an intrinsic death rate and competition modifying birth rates will be studied elsewhere.

The system is characterized by the vector of probabilities $P(s, t \mid s^0)$ to be in a state $s = \{x_1, x_2\}$ at time t, given the initial conditions $s^0 = (x_1^0, x_2^0)$: $[P](t) \equiv (\cdots, P(s, t|s^0), \cdots)$ [86]. The forward master equation describing the time evolution of this probability distribution is [81]

$$\frac{\mathrm{d}}{\mathrm{d}t}[P](t) = \hat{M}[P](t), \tag{3.2}$$

where $\hat{M}$ is the (semi-infinite) transition matrix, with more details given in the following paragraph.

Because the approximate analytical and semi-analytical solutions of the master equation (3.2) often do not provide correct scaling in all regimes ([85,87–89]; see also the electronic supplementary material), we analyse the master equation numerically in order to recover both the exponential and polynomial aspects of the mean time to fixation. To enable numerical manipulations, we introduce a reflecting boundary condition at a cut-off population size $C_K > K$ for both species to make the transition matrix finite [86,90,91] and enumerate the states of the system with a single index [86] via the mapping of the two species populations (x_1, x_2) to state s as

$$s(x_1, x_2) = (x_1 - 1)C_K + x_2 - 1, \tag{3.3}$$

where s serves as the index for our concatenated probability vector.

In this representation, the non-zero elements of the sparse matrix $\hat{M}$ are $\hat{M}_{s,s} = -b_1(s) - b_2(s) - d_1(s) - d_2(s)$ along the diagonal, giving the rate of transition out of state (x_1, x_2) to the adjacent states $(x_1 + 1, x_2)$, $(x_1, x_2 + 1)$, $(x_1 - 1, x_2)$ or $(x_1, x_2 - 1)$, respectively, corresponding to a species 1 or 2 birth or death event. Off the diagonal, the elements $\hat{M}_{s,s+1} = d_2(s + 1)$ give the transition rate from the state of populations (x_1, x_2) of the two species to the state $(x_1, x_2 - 1)$ organisms, corresponding to the death of a member of species 2. Off-diagonal elements $\hat{M}_{s+1,s} = b_2(s)$ are the transition from state (x_1, x_2) to state $(x_1, x_2 + 1)$, similarly corresponding to the birth of an organism from species 2. The off-diagonal elements at $\pm C_K$ are the remaining two transitions: the death of species 1 member is given by $\hat{M}_{s,s+C_K} = d_1(s + C_K)$, and its birth is $\hat{M}_{s+C_K,s} = b_1(s)$. Some diagonal elements are modified to ensure the reflecting boundary at $x_i = C_K$. We have found that the choice $C_K = 5K$ is more than sufficient to calculate the mean fixation times to at least three significant digits of accuracy.

3.1. Fixation time as a function of the niche overlap

In this section, we calculate the first passage times to the extinction of one of the species and the corresponding fixation of the other, induced by demographic fluctuations, starting from an initial condition of the deterministically stable coexistence point. The stochastic system tends to fluctuate near the deterministic fixed point (or Moran line), but rare fluctuations can take the system far from equilibrium. Should the fluctuations bring the system to either of the axes, then one species has gone extinct. In this model, each axis acts as an absorbing manifold, from which the system cannot recover. Biologically, once a species has gone extinct from the system it can no longer reproduce. The system then proceeds to evolve as a one species logistic model with demographic noise, a process that is well studied in the literature [59,62,92].

The time the system takes to fixation is a random variable, the distribution of which can be calculated in a number of ways. The master equation (3.2) has a formal solution obtained by the exponentiation of the matrix: $[P](t) = \mathrm{e}^{\hat{M}t}[P](0)$. Then $([P])_{s=(x_1,0)}$ and $([P])_{s=(0,x_2)}$ give the cumulative distribution of the fixation of species 1 and 2, respectively. However, direct matrix exponentiation, as well as direct sampling of the master equation using the Gillespie algorithm [93,94], are impractical, since the fixation time grows exponentially with the system size; nevertheless, we used Gillespie tau-leaping simulations to verify our results up to moderate system size (see electronic supplementary material). More amenably, the moments of the first passage time distribution can be calculated directly without explicitly solving the master equation [95]. In an ensemble of trajectories, the fraction of trajectories in state s at time t is given by $P(s, t|s^0)$. Thus, averaging over the ensemble, the mean residence time in state s during the system evolution is the integral of this quantity over all time [95]

$$\langle t(s^0) \rangle_s = \int_0^\infty \mathrm{d}t\, P(s, t|s^0) = \int_0^\infty \mathrm{d}t\, (\mathrm{e}^{\hat{M}t})_{s,s^0} = -(\hat{M}^{-1})_{s,s^0}. \tag{3.4}$$
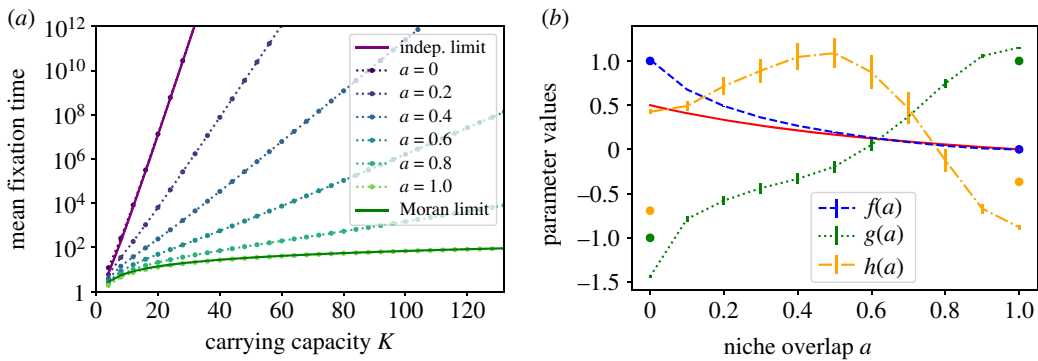
Figure 2. (a) Dependence of the fixation time on carrying capacity and niche overlap. The lowest line, $a = 1$, recovers the Moran model results with the fixation time algebraically dependent on K for $K \gg 1$. For all other values of a, the fixation time is exponential in K for $K \gg 1$. (b) Niche overlap controls the transition from coexistence to fixation. Blue line: $f(a)$ from the ansatz of equation (3.6) characterizes the exponential dependence of the fixation time on K; it smoothly approaches zero as the niche overlap reaches its Moran line value $a = 1$. Green line: $g(a)$ quantifies the scaling of the pre-exponential prefactor $K^{g(a)}$ with K. Yellow line: $h(a)$ is the multiplicative constant. The bars represent a 95% confidence interval, and for f are thinner than the line. The dots at the extremes $a = 0$ and $a = 1$ are the expected asymptotic values. Red line: Gaussian approximation to Fokker–Planck equation (see next subsection).

For each trajectory, the time to reach fixation is simply the sum of the times it spends in each state on the way. Thus the mean time to fixation starting from a state s^0 is the sum of the residency times [96]

$$\tau(s^0) = -\sum_s \langle t(s^0) \rangle_s = -\sum_s (\hat{M}^{-1})_{s,s^0}. \tag{3.5}$$

This expression can also be derived using the backward master equation formalism [96]. The matrix inversion was performed using LU decomposition algorithm implemented with the C++ library Eigen [97], which has algorithmic complexity of the calculation scaling algebraically with K. Increasing the cut-off C_K enables calculation of the mean fixation times to an arbitrary accuracy.

Figure 2a shows the calculated fixation times with the initial condition at the deterministically stable coexistence fixed point as a function of the carrying capacity K for different values of the niche overlap a. While the transition has not previously been characterized, the independent and neutral limits are known, providing comparisons at the $a = 0$ and $a = 1$ extremes.

In the limit of non-interacting species ($a = 0$), each species evolves according to an independent stochastic logistic model, and the probability distribution of the fixation times is a convolution of the extinction time distributions of a single species, which are dominated by a single exponential tail [59,62,92] (see also the electronic supplementary material). Mean extinction time of a single species can be calculated exactly and is well known, and asymptotically for $K \gg 1$ it varies as $1/Ke^K$ [98,99]. Denoting the probability distribution of the extinction times for either of the independent species starting from K asymptotically for large K as $p(t) = \alpha e^{-\alpha t}$ and its cumulative as $f(t) = \int_{s=0}^t p(s)\,ds$, the probability that *either* of the species goes extinct in the time interval $[t, t + dt]$, is $p_{min}(t)\,dt = (p(t)(1 - f(t)) + (1 - f(t))p(t))\,dt$. Thus the mean time to fixation is $\langle t \rangle = \int_0^\infty dt\, t\, p_{min}(t) = 1/2\alpha$, where $1/\alpha = (1/K)e^K$ is the mean time of the single species extinction. This analytical limit $\tau \simeq (1/2K)e^K$ is shown in figure 2 as a solid purple line and agrees well with the numerical results of equation (3.5). From the biological perspective, for sufficiently large K, the exponential dependence of the fixation time on K implies that the fluctuations do not destroy the stable coexistence of the two species.

In the opposite limit of the complete niche overlap, $a = 1$, any fluctuations along the line of neutrally stable points are not restored, and the system performs diffusion-like motion that closely parallels the random walk of the classic Moran model [38,43,49,54,56,57,74] (see also the electronic supplementary material). The Moran model shows a relatively fast fixation time scaling algebraically with K [42,43], $\tau \simeq \ln(2)K^2 \Delta t$, where Δt is one-time step of a Moran model in our non-dimensionalized time units. This known result can be obtained from the backward Fokker–Planck equation $\partial^2 \tau / \partial x^2 = -\Delta t K^2 / x(K - x)$ of the Moran model, which directly gives the above scaling for equal population initial conditions [42,43]. The fixation time predicted by the Moran model is shown in figure 2 as a green solid line and shows excellent agreement with our exact result. Note that the average time step Δt in the corresponding Moran model is $\Delta t \approx 1/K$ because the mean transition time in the stochastic LV model

is proportional to $1/(rK)$ close to the Moran line [57]; see the electronic supplementary material for more details. The relatively short fixation time in the complete niche overlap regime implies that the population can reach fixation on biologically realistic timescales.

The exponential scaling of the fixation time with K persists for incomplete niche overlap described by the intermediate values of $0 < a < 1$. However, both the exponential and the algebraic prefactor depend on the niche overlap a. The exponential scaling is expected for systems with a deterministically stable fixed point [38,55,62,88,89], as indicated in [43,54,57] using Fokker–Planck approximation and in [55,100,101] using the Wentzel–Kramers–Brillouin (WKB) approximation. However, the Fokker–Planck and WKB approximations, while providing the qualitatively correct dominant scaling, do not correctly calculate the scaling of the polynomial prefactor and the numerical value of the exponent simultaneously [62,74,85]. For large population sizes and timescales, effective species coexistence will be typically observed experimentally whenever the fixation time has a non-zero exponential component.

To quantitatively investigate the transition from the exponentially stable fixation times to the algebraic scaling in the complete niche overlap regime, we use the ansatz

$$\tau(a, K) = e^{h(a)} K^{g(a)} e^{f(a)K}. \tag{3.6}$$

In the Moran limit, $a = 1$, we expect $f(1) = 0$, $g(1) = 1$. In the independent species limit with zero niche overlap, $a = 0$, we expect $f(0) = 1$ and $g(0) = -1$. Figure 2b shows the ansatz functions $f(a)$, $g(a)$ and $h(a)$, obtained by numerical fit to the fixation times as a function of K shown in figure 2a.

The numerical results agree well with the expected approximate analytical results for $a = 0$ and $a = 1$ with small discrepancies attributable to the approximate nature of the limiting values. Notably, $f(a)$, which quantifies the exponential dependence of the fixation time on the niche overlap a, smoothly decays to zero at $a = 1$: only when two species have complete niche overlap ($a = 1$) does one expect rapid fixation dominated by the algebraic dependence on K. In all other cases, the mean time until fixation is exponentially long in the system size [62,92]. Even two species that occupy *almost* the same niche ($a \lesssim 1$) effectively coexist for $K \gg 1$, with small fluctuations around the deterministically stable fixed point; for a discussion of small K, see the next paragraph and electronic supplementary material. The dependence of the exponential function $e^{f(a)K}$ on a and K can be understood in the spirit of Kramers' theory, as discussed in the next section.

Interestingly, for small K the algebraic prefactors may dominate the exponential scaling such that in a region of a and K space, the fixation time from a deterministically stable fixed point (with $a < 1$) can be shorter than that of a Moran case with the same K. See the electronic supplementary material for more details. Also explored in the electronic supplementary material is a breaking of the parameter symmetry, which gives similar behaviour to the above. In particular, the exponential dependence of the escape time from the fixed point on the system size also persists in the non-neutral case, although the dependence can be much weaker.

3.2. Route to fixation and the origin of the exponential scaling

To gain deeper insight into the fixation dynamics and to understand the origins and the limits of the exponential scaling with K, in this section, we calculate the residency times in each state during the fixation process, given by equation (3.4). The results are shown as a contour plot in figure 3, for two different niche overlaps, one at and the other far from the Moran limit. The set of states lying along the steepest descent lines of the contour plot, shown as the black line, can be thought of as a 'typical' trajectory [55,74,102]. However, even for two species close to complete niche overlap the system trajectory visits many states far from this line. This departure is even greater for weakly competing species, where the system covers large areas around the fixed point before the rare fluctuation that leads to fixation occurs [53]. These deviations from a 'typical' trajectory are related to the inaccuracy of the WKB approximation in calculating the scaling of the pre-exponential factor [53,89,99]; see also the electronic supplementary material. This occupancy landscape can be qualitatively thought of as an effective Lyapunov function/effective potential of the system dynamics [103], although the LV system does not possess a true Lyapunov function.

A similar issue also arises in the Fokker–Planck approximation [57,103]. Nevertheless, the pseudo-potential (also known as quasi-potential) landscape provides an intuitive underpinning for the general exponential scaling in the incomplete niche overlap regime: the fixation process can be thought of as the Kramers-type escape from a pseudo-potential well [104]. The Kramers' escape time is dominated by the exponential term $\tau \simeq \exp(\Delta U)$, where ΔU is the depth of the effective potential well, corresponding to the dominant scaling $\tau \simeq \exp(f(a)K)$ of this paper. The depth of the pseudo-potential
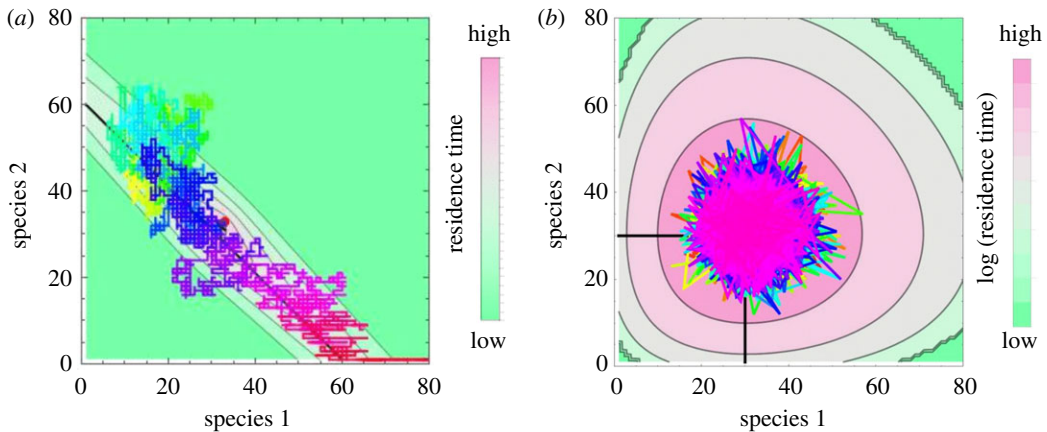
Figure 3. The system samples multiple trajectories on its way to fixation. Contour plot shows the average residency times at different states of the system, with pink indicating longer residence time, green indicating rarely visited states. The coloured line is a sample trajectory the system undergoes before fixation; colour coding corresponds to the elapsed time, with orange at early times, purple at the intermediate times and red at late stages of the trajectory. The red dot shows the deterministic coexistence point. See text for more details. (a) Complete niche overlap limit, $a = 1$, for $K = 64$. (b) Independent limit with $a = 0$ and $K = 32$.

well can be estimated in the Gaussian approximation to the Fokker–Planck equation [81,105,106]. For $y_i \equiv x_i/K$, the Fokker–Planck equation is $\partial_t P = -\sum_i \partial_i F_i P + (1/2K)\sum_{i,j}\partial_i\partial_j D_{ij}P$ with $F_1 = y_1(1 - y_1 - a\,y_2)$, $D_{11} = y_1\,(1 + y_1 + a\,y_2)$, similar terms for F_2 and D_{22}, and $D_{12} = D_{21} = 0$. Linearized about the deterministic fixed point $[y]^*$ the Fokker–Planck equation becomes $\partial_t P = -\sum_{i,j} A_{ij}\partial_i(y_j - y_j^*)P + (1/2K)\sum_{i,j}B_{ij}\partial_i\partial_j P$, where $A_{ij} = \partial_j F_i|_{[y]=[y]^*}$ and $B_{ij} = D_{ij}|_{[y]=[y]^*}$. The steady-state solution to this approximation is a Gaussian distribution centred on the deterministic fixed point. It gives an effective well depth of $\Delta U = ((1-a)/2(1+a))K$, providing a qualitative basis for the numerical results in figure 2b. As a increases and the species interact more strongly, the potential well becomes less steep, resulting in weaker exponential scaling. In the complete niche overlap limit, the pseudo-potential develops a soft direction along the Moran line that enables relatively fast escape towards fixation. The change in the topology of the pseudo-potential is also reflected in the Pearson correlation coefficient between the two species: $\rho = \mathrm{cov}(x_1, x_2)/\sqrt{\sigma_1^2\sigma_2^2} = -a$. The covariance ranges from zero in the independent limit (as expected) to anti-correlated in the Moran limit, reflecting the fact that the trajectories typically diffuse along the trough around the Moran line.

3.3. Invasion of a mutant/immigrant into a deterministically stable population

Transient coexistence during the fixation/extinction process of immigrants/mutants has also been proposed as a mechanism for observed biodiversity in a number of contexts [31,35,70,73,75,107,108]. The extent of this biodiversity is constrained by the interplay between the residence times of these invaders and the rate at which they appear in a settled population. In the previous sections, we calculated the fixation times in the two-species system starting from the deterministically stable fixed point. In this section, we investigate the complementary problem of robustness of a stable population of one species with respect to an invasion of another species, arising either through mutation or immigration, and investigate the effect of niche overlap and system size on the probability and mean times of successful and failed invasions.

To this end, we study the case where the system starts with $K - 1$ individuals of the established species and 1 invader. Each species' dynamics is described by the birth and death rates defined by equations (3.1) above. We consider the invasion successful if the invader grows to be half of the total population without dying out first. Note that this is different from the bulk of invasion literature [43,49,54–58,64,70,90,107,109–112] (but see [113]), which typically considers invasion successful when a mutant fixates in the system. However, this is only sensible in the Moran limit, since otherwise the system tends to the coexistence fixed point, after which there is an equal chance of fixation and extinction, with the MTE calculated above; hence our definition of invasion. We denote the probability of a invader success as $\mathcal{P}$, the mean time to a successful invasion as τ_s, and the mean time of a failed invasion attempt, where the invader dies out before establishing itself in the population, as τ_f. More
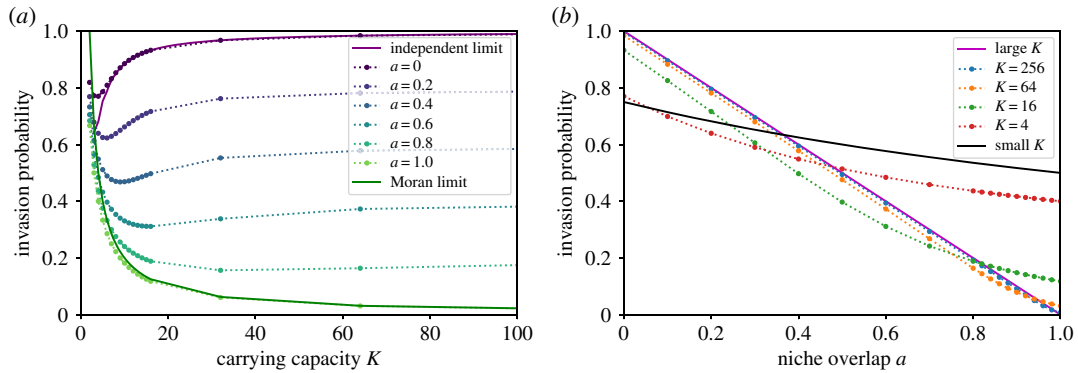
Figure 4. Probability of a successful invasion. (a) Solid lines show the numerical results, from $a = 0$ at the top to $a = 1$ at the bottom. The purple solid line is the expected analytical solution in the independent limit. The green solid line is the prediction of the Moran model in the complete niche overlap case. Numerical data are obtained using equation (3.7) and are connected with dotted lines to guide the eye. (b) The red dotted line shows the results for carrying capacity $K = 4$, the solid black line $\frac{b_{mut}}{b_{mut} + d_{mut}}$ is an appropriate analytical approximation in the small carrying capacity limit. Successive lines are at larger system sizes, and approach the solid magenta line of $1 - d_{mut}/b_{mut} \approx 1 - a$ at very large K.

generally, invasion probability and the successful and failed times starting from an arbitrary state s^0 are denoted as $\mathcal{P}^{s^0}$, $\tau_s^{s^0}$ and $\tau_f^{s^0}$, respectively.

Similar to equation (3.5) above, the invasion probability can be obtained from [96,105]

$$\mathcal{P}^{s^0} = -\sum_s \hat{M}_{s,s^0}^{-1} \alpha_s \tag{3.7}$$

and the times from

$$\Phi^{s^0} = -\sum_s \hat{M}_{s,s^0}^{-1} \mathcal{P}^s, \tag{3.8}$$

where α_s is the transition rate from a state s directly to extinction or invasion of the invader and $\Phi^{s^0} = \tau^{s^0} \mathcal{P}^{s^0}$ is a product of the invasion or extinction time and probability. Similar equations describe τ_f [96,105].

Figure 4 shows the calculated invasion probabilities as a function of the carrying capacity K and of the niche overlap a between the invader and the established species. In the complete niche overlap limit, $a = 1$, the dependence of the invasion probability on the carrying capacity K closely follows the results of the classical Moran model, $\mathcal{P}^{s^0} = 2/K$ [42,90], shown in the solid green line in figure 4a, and tends to zero as K increases. In the other limit, $a = 0$, the problem is well approximated by the one-species stochastic logistic model starting with one individual and evolving to either 0 or K individuals; the exact result in this limit is shown as a black dotted line, referred to as the independent limit [105]. In the independent limit, $a = 0$, the invasion probability asymptotically approaches 1 for large K, reflecting the fact that the system is deterministically drawn towards the deterministic stable fixed point with equal numbers of both species. Interestingly, the invasion probability is a non-monotonic function of K and exhibits a minimum at an intermediate/low carrying capacity, which might be relevant for some biological systems, such as in early cancer development [13] or plasmid exchange in bacteria [17]. The explanation for this non-monotonicity is that increasing K has opposing effects: it makes the end goal of growing from one invader to half the population farther away, but it also increases the effective draw towards the deterministic fixed point.

For the intermediate values of the niche overlap, $0 < a < 1$, the invasion probability is a monotonically decreasing function of a, as shown in figure 4b. For large K, the outcome of the invasion is typically determined after only a few steps: since the system is drawn deterministically to the mixed fixed point, the invasion is almost certain once the invader has reproduced several times. At early times, the invader birth and death rates (3.1) are roughly constant, and the invasion failure can be approximated by the extinction probability of a birth–death process with constant death d_{mut} and birth b_{mut} rates. The invasion probability is then $\mathcal{P} = 1 - d_{mut}/b_{mut} \approx 1 - a$. This heuristic estimate is in excellent agreement with the numerical predictions, shown in figure 4b as a solid magenta and the dotted blue lines, respectively. For this reason, at large K, the dependence of the invasion probability on a is much stronger than its dependence on K, such that increasing the carrying capacity has little
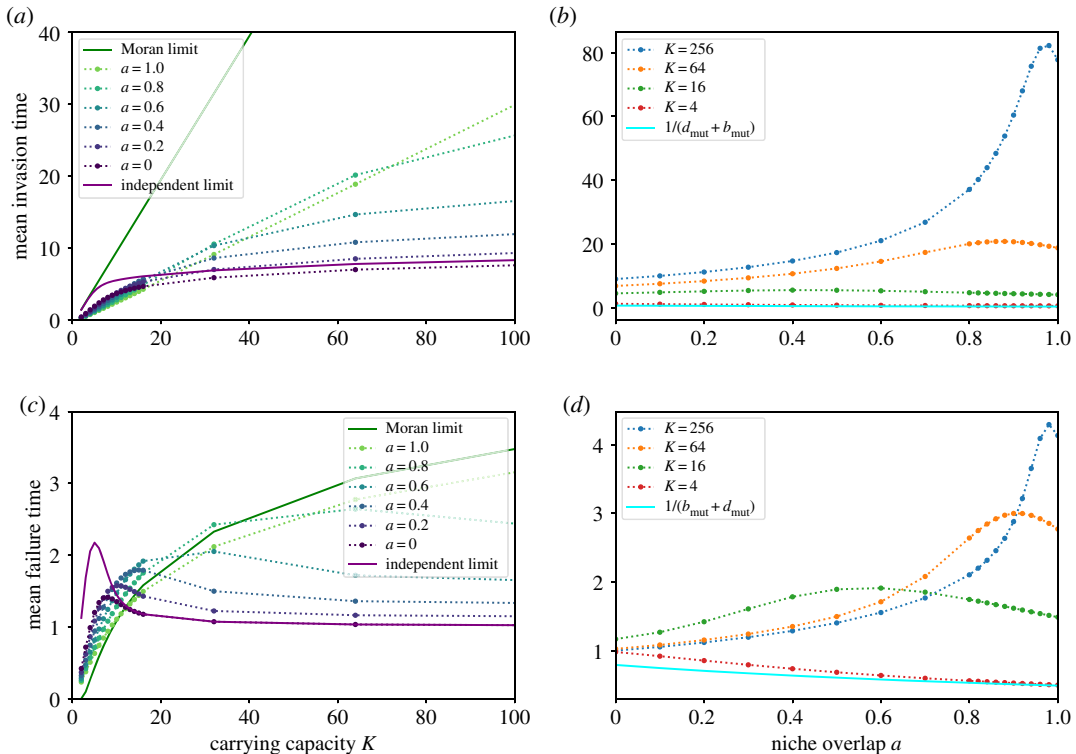
Figure 5. Mean time of a successful or failed invasion attempt. (*a*) Dotted lines show the numerical results of invasion times conditioned on success, from $a = 0$ at the bottom being mostly fastest to $a = 1$ being slowest. The solid green line shows for comparison the predictions of the Moran model in the complete niche overlap limit, $a = 1$; see text. The solid purple line corresponds to the solution of independent stochastic logistic species, $a = 0$, and overestimates the time at small K but fares better as K increases. (*b*) The red dotted line shows the successful invasion times for carrying capacity $K = 4$, and successive lines are at larger system sizes, up to $K = 256$. The cyan line is $1/(b_{mut} + d_{mut})$ and matches with numerical results at small K. (*c,d*) Same as upper panels, but for the mean time conditioned on a failed invasion attempt.

effect on the eventual outcome of the system, but a small change in the niche overlap between the invader and the established species leads to a large change in the probability of invasion success. For small K, either invasion or extinction typically occurs after only a small number of steps. The invasion probability in this limit is dominated by the probability that the lone mutant reproduces before it dies, namely $b_{mut}/b_{mut} + d_{mut} = K/(K(1 + a) + 1 - a)$, as shown in black solid line in figure 4*b*.

Figure 5*a* shows the dependence of the mean time to successful invasion, τ_s, on K and a. Increasing K can have potentially contradictory effects on the invasion time, as it increases the number of births before a successful invasion on the one hand, while increasing the steepness of the potential landscape and therefore the bias towards invasion on the other. Nevertheless, the invasion time is a monotonically increasing function of K for all values of a. In the complete niche overlap limit $a = 1$, the invasion time scales linearly with the carrying capacity K, as expected from the predictions of the Moran model, $\tau_s = \Delta t \ K^2(K - 1)\ln(K/(K - 1))$ with $\Delta t \simeq 1/K$, as explained above. The quantitative discrepancy arises from the breakdown of the $\Delta t \simeq 1/K$ approximation off the Moran line. In the opposite limit of non-interacting species, $a = 0$, the invading mutant follows the dynamics of a single logistic system with the carrying capacity K, resulting in the invasion time that grows approximately logarithmically with the system size, as shown in figure 5*a,c* as a solid purple line (see also electronic supplementary material). For all values $0 \leq a < 1$, the invasion time scales sublinearly with the carrying capacity, indicating that successful invasions occur relatively quickly, even when close to complete niche overlap, where the invading mutant strongly competes against the stable species.

By contrast, the failed invasion time, shown in figure 5*c*, is non-monotonic in K. The analytical approximations of the Moran model and of the two independent one-dimensional stochastic logistic systems recover the qualitative dependence of the failed invasion time on K at high and low niche overlap, respectively. All failed invasion times are fast, with the greatest scaling being that of the Moran limit. For $a < 1$, these failed invasion attempts approach a constant timescale at large K.

The dependence of the time of an attempted invasion (both for successful and failed ones) on the niche overlap a is different for small and large K, as shown in figure 5b,d. For small K, both τ_s and τ_f are monotonically decreasing functions of a, with the Moran limit having the shortest conditional times. In this regime, the extinction or fixation already occurs after just a few steps, and its timescale is determined by the slowest steps, namely the mutant birth and death. Thus $\tau \approx 1/(b_{\mathrm{mut}} + d_{\mathrm{mut}}) = K/(K + 1 + a(K-1))$, as shown in the figures as the solid cyan line. By contrast, at large K, the invasion time is a non-monotonic function of the niche overlap, increasing at small a and decreasing at large a. This behaviour stems from the conflicting effect of the increase in niche overlap: on the one hand, increasing a brings the fixed point closer to the initial condition of one invader, suggesting a shorter timescale; on the other hand, it also makes the two species more similar, increasing the competition that hinders the invasion.

4. Discussion

Maintenance of species biodiversity in many biological communities is still incompletely understood. The classical idea of competitive exclusion postulates that ultimately only one species should exist in an ecological niche, excluding all others. Although the notion of an ecological niche has eluded precise definition, it is commonly related to the limiting factors that constrain or affect the population growth and death. In the simplest case, one factor corresponds to one niche, which supports one species, although a combination of factors may also define a niche, as discussed above. The competitive exclusion picture has encountered long-standing challenges as exemplified by the classical 'paradox of the plankton' [4,35] in which many species of plankton seem to cohabit the same niche; in many other ecosystems the biodiversity is also higher than appears to be possible from the apparent number of niches [31,35,39,114,115].

Competitive exclusion-like phenomena appear in a number of popular mathematical models, for instance in the competition regime of the deterministic LV model, whose extensive use as a toy model enables a mathematical definition of the niche overlap between competing populations [26–29]. Another classical paradigm of fixation within an ecological niche is the Moran model (and the closely related Fisher–Wright, Kimura and Hubbell models) that underlies a number of modern neutral theories of biodiversity [19,20,31,42–45]. Unlike the deterministic models, in the Moran model fixation does not rely on the deterministic exclusion of one species by the other, like in the strong competition and bistable regimes of the stability diagram figure 1 of the electronic supplementary material. Recently, the connection between deterministic models of the LV type and stochastic models of the Moran type has accrued renewed interest because of new focus on the stochastic dynamics of the microbiome, immune system, and cancer progression [13,25,43,49,56,57,73,89].

Much of the recent studies of these systems employed various approximations, such as the Fokker–Planck approximation [38,43,54,56,57], WKB approximation [55,74] or game-theoretic [49] approach. The results of these approximations typically differ from the exact solution of the master equation, used in this paper, especially for small population sizes [62,74,85,88,89]. In this paper, we have interrogated stochastic dynamics of a system of two competing species using a numerically arbitrarily accurate method based on the first passage formalism in the master equation description. The algorithmic complexity of this method scales algebraically with the population size rather than with the exponential scaling of the fixation time (as is the case with the Gillespie algorithm [93]). Our approach captures both the exponential terms and the algebraic prefactors in the fixation/extinction times for all population sizes and enables us to rigorously investigate the effect of niche overlap between the species on the transition between the known limits of the effectively stable and the stochastically unstable regimes of population diversity.

Stochastic fluctuations allow the system to escape from the deterministic coexistence fixed point towards fixation. If the escape time is exponential in the (typically large) system size, in practice it implies effective coexistence of the two species around their deterministic coexistence point. If the escape time is algebraic in K, as in the degenerate niche overlap case (closely related to the classical Moran model), the system may fixate on biological timescales [42,107]. Nevertheless, for biological systems with small characteristic population sizes, exponential scaling may not dominate the fixation time, and the algebraic prefactors dictate the behaviour of the system (see the electronic supplementary material for more details).

The transition from the exponential scaling of the effective coexistence time to the rapid stochastic fixation in the Moran limit is governed by the niche overlap parameter. We find that the fixation time

is exponential in the system size unless the two species occupy exactly the same niche. The numerical factor in the exponential is highly sensitive to the value of the niche overlap, and smoothly decays to zero in the complete niche overlap case. The implication is that two species will effectively coexist unless they have exactly the same niches.

Our fixation time results can be understood by noticing that the escape from a deterministically stable coexistence fixed point can be likened to Kramers' escape from a pseudo-potential well [54,62,92,116], where the mean transition time grows exponentially with well depth [62]. Approximating the steady-state probability with a Gaussian distribution shows that this well depth is proportional to $K(1-a)$ and disappears at $a = 1$. With complete niche overlap, the system develops a 'soft' marginally stable direction along the Moran line that enables algebraically fast escape towards fixation [54,57,90]. Similar to the exponential term, the exponent of the algebraic prefactor is also a function of the niche overlap and smoothly varies from -1 in the independent regime of non-overlapping niches to $+1$ in the Moran limit.

The fixation times of two coexisting species, discussed above, determine the timescales over which the stability of the mixed populations can be destroyed by stochastic fluctuations. Similarly, the times of successful and failed invasions into a stable population set the timescales of the expected transient coexistence in the case of an influx of invaders, arising from mutation, speciation or immigration. The probability of invasion strongly depends on the niche overlap, and for large K decreases monotonically as $1 - a$ with the increase in niche overlap. By contrast, the effect of the carrying capacity on the invasion probability is negligible in the large K limit.

The mean times of both successful and failed invasions are relatively fast in all regimes, and scale linearly or sublinearly with the system size K. Even for high niche overlap, where the invasion probability is low due to the strong competition between the species, those invaders who do succeed invade in a reasonably fast time. In this high competition regime, the times of the failed invasions are particularly salient because they set the timescales for transient species diversity. If the influx of invaders is slower than the mean time of their failed invasion attempts, most of the time the system will contain only one settled species, with rare 'blips' corresponding to the appearance and quick extinction of the invader. On the other hand, if individual invaders arrive faster than the typical times of extinction of the previous invasion attempt, the new system will exhibit transient coexistence between the settled species and multiple invader strains, determined by the balance of the mean failure time and the rate of invasion [26,31,35,108].

The weaker dependence of the invasion times on the population size and the niche overlap, when compared with the escape times of a stably coexisting system to fixation, implies that the transient coexistence is expected to be much less sensitive to the niche overlap and the population size than the steady-state coexistence. Of note, both niche overlap and the population size can have contradictory effects on the invasion times (as discussed in §3) resulting in a non-monotonic dependence of the times of both successful and failed invasions on these parameters.

Our results indicate that the niche overlap between two species reflecting the similarity (or the divergence) in how they interact with their shared environment, is of critical importance in determining stability of mixed populations. This has important implications for understanding the long-term population diversity in many systems, such as human microbiota in health and disease [2,3,12], industrial microbiota used in fermented products [16], and evolutionary phylogeny inference algorithms [14,15]. Our results serve as a neutral model base for problems such as maintenance of drug resistance plasmids in bacteria [17] or strain survival in cancer progression [13]. The theoretical results can also be tested and extended based on experiments in more controlled environments, such as the gut microbiome of a *C. elegans* [73], or in microfluidic devices [117].

The results of the paper can also inform investigations of multi-species systems [24–26,30–32,35–38,69,90,118,119]. It is helpful to focus on one of the species within a large community of different species, which experiences a distribution of niche overlaps with other species in the system. Since extinction times away from complete niche overlap scale exponentially in the system size, the extinction of the given species is likely to be dominated by the shortest timescale, imposed by whichever other species has the greatest niche overlap with it, excluding it most strongly. Therefore, species extinctions are expected to occur more frequently in communities where the probability of high niche overlap between the species is high—for instance for distributions with high mean overlap, or high variance in the niche overlap distribution. These qualitative predictions compare favourably with the work of Capitán *et al.* [30], which shows that increasing the niche overlap in a multi-species system results on average in a smaller number of coexisting species, decreasing biodiversity. The probability of invasion into a multi-species system is more complicated than the coexistence

considerations, because, unlike the fixation times, invasion times do not scale exponentially with the system size, so no single pairwise interaction will dominate the timescale. These directions are beyond of the scope of the present work and will be studied elsewhere.

Authors' contributions. M.B. and A.Z. designed the research, M.B. performed the research, M.B. and A.Z. wrote the paper. All authors gave final approval for publication.

References

1. Korem T et al. 2015 Growth dynamics of gut microbiota in health and disease inferred from single metagenomic samples. Science 349, 1101–1106. (doi:10.1126/science.aac4812)

2. Coburn B et al. 2015 Lung microbiota across age and disease stage in cystic fibrosis. Sci. Rep. 5, 10241. (doi:10.1038/srep10241)

3. Palmer J, Kazmerzak K, Hansen MC, Kolenbrander PE. 2001 Mutualism versus independence: strategies of mixed-species oral biofilms in vitro using saliva as the sole nutrient source. Infect. Immun. 69, 5794–5804. (doi:10.1128/IAI.69.9.5794-5804.2001)

4. Hutchinson GE. 1961 The paradox of the plankton. Am. Nat. 95, 137–145. (doi:10.1086/282171)

5. Cordero OX, Datta MS. 2016 Microbial interactions and community assembly at microscales. Curr. Opin. Microbiol. 31, 227–234. (doi:10.1016/j.mib.2016.03.015)

6. Friedman J, Higgins LM, Gore J. 2017 Community structure follows simple assembly rules in microbial microcosms. Nat. Ecol. Evol. 1, 0109. (doi:10.1038/s41559-017-0109)

7. Weinstein JA, Jiang N, White RA, Fisher DS, Quake SR. 2009 High-throughput sequencing of the zebrafish antibody repertoire. Science 324, 807–810. (doi:10.1126/science.1170020)

8. Desponds J, Mora T, Aleksandra W. 2015 Fluctuating fitness shapes the clone size distribution of immune repertoires. Proc. Natl Acad. Sci. USA 113, 1–17. (doi:10.1101/021923)

9. Stirk ER, Lythe G, Molina-Paris C. 2010 Stochastic competitive exclusion in the maintenance of the naive T cell repertoire. J. Theor. Biol. 265, 396–410. (doi:10.1016/j.jtbi.2010.05.004)

10. Tilman D. 1996 Biodiversity: population versus ecosystem stability. Ecology 77, 350–363. (doi:10.2307/2265614)

11. Naeem S et al. 2001 Biodiversity and ecosystem functioning: current knowledge and future challenges. Science 294, 804–808. (doi:10.1126/science.1064088)

12. Kinross JM, Darzi AW, Nicholson JK. 2011 Gut microbiome-host interactions in health and disease. Genome Med. 3, 14. (doi:10.1186/gm228)

13. Ashcroft P, Michor F, Galla T. 2015 Stochastic tunneling and metastable states during the somatic evolution of cancer. Genetics 199, 1213–1228. (doi:10.1534/genetics.114.171553)

14. Rice SH. 2004 Evolutionary theory: mathematical and conceptual foundations. Sunderland, MA: Sinauer Associates.

15. Blythe RA, McKane AJ. 2007 Stochastic models of evolution in genetics, ecology and linguistics. J. Stat. Mech: Theory Exp. 2007, P07018. (doi:10.1088/1742-5468/2007/07/P07018)

16. Wolfe BE, Button JE, Santarelli M, Dutton RJ. 2014 Cheese rind communities provide tractable systems for in situ and in vitro studies of microbial diversity. Cell 158, 422–433. (doi:10.1016/j.cell.2014.05.041)

17. Gooding-Townsend R, Ten Holder S, Ingalls B. 2015 Displacement of bacterial plasmids by engineered unilateral incompatibility. IEEE Life Sci. Lett. 1, 19–21. (doi:10.1109/LLS.2015.2465839)

18. Hardin G. 1960 The competitive exclusion principle. Science 131, 1292–1297. (doi:10.1126/science.131.3409.1292)

19. Mayfield MM, Levine JM. 2010 Opposing effects of competitive exclusion on the phylogenetic structure of communities. Ecol. Lett. 13, 1085–1093. (doi:10.1111/j.1461-0248.2010.01509.x)

20. Kimura M, Ohta T. 1969 The average number of generations until fixation of a mutant gene in a finite population. Genetics 61, 763.

21. Nadell CD, Bucci V, Drescher K, Levin Sa, Bassler BL, Xavier JB. 2013 Cutting through the complexity of cell collectives. Proc. R. Soc. B 280, 20122770. (doi:10.1098/rspb.2012.2770)

22. Armstrong RA, McGehee R. 1976 Coexistence of species competing for shared resources. Theor. Popul. Biol. 9, 317–328. (doi:10.1016/0040-5809(76)90051-4)

23. McGehee R, Armstrong RA. 1977 Some mathematical problems concerning the ecological principle of competitive exclusion. J. Differ. Equ. 23, 30–52. (doi:10.1016/0022-0396(77)90135-8)

24. Armstrong RA, McGehee R. 1980 Competitive exclusion. Am. Nat. 115, 151–170. (doi:10.1086/283553)

25. Posfai A, Taillefumier T, Wingreen NS. 2017 Metabolic trade-offs promote diversity in a model ecosystem. Phys. Rev. Lett. 118, 028103. (doi:10.1103/PhysRevLett.118.028103)

26. MacArthur R, Levins R. 1967 The limiting similarity, convergence, and divergence of coexisting species. Am. Nat. 101, 377–385. (doi:10.1086/282505)

27. Abrams P. 1980 Some comments on measuring niche overlap. Ecology 61, 44–49. (doi:10.2307/1937153)

28. Schoener TW. 1985 Some comments on Connell's and my reviews of field experiments on interspecific competition. Am. Nat. 125, 730–740. (doi:10.1086/284375)

29. Chesson P, Kuang JJ. 2008 The interaction between predation and competition. Nature 456, 235–238. (doi:10.1038/nature07248)

30. Capitán JA, Cuenda S, Alonso D. 2015 How similar can co-occurring species be in the presence of competition and ecological drift? J. R. Soc. Interface 12, 20150604. (doi:10.1098/rsif.2015.0604)

31. Hubbell SP. 2001 The unified theory of biodiversity and biogeography. Princeton, NJ: Princeton University Press.

32. Desai MM, Fisher DS. 2007 Beneficial mutation-selection balance and the effect of linkage on positive selection. Genetics 176, 1759–1798. (doi:10.1534/genetics.106.067678)

33. Carroll IT, Nisbet RM. 2015 Departures from neutrality induced by niche and relative fitness differences. Theor. Ecol. 8, 449–465. (doi:10.1007/s12080-015-0261-0)

34. Leibold MA. 1995 The niche concept revisited: mechanistic models and community context. Ecology 76, 1371–1382. (doi:10.2307/1938141)

35. Chesson P. 2000 Mechanisms of maintenance of species diversity. Annu. Rev. Ecol. Syst. 31, 343–366. (doi:10.1146/annurev.ecolsys.31.1.343)

36. Adler PB, Ellner SP, Levine JM. 2010 Coexistence of perennial plants: an embarrassment of niches. Ecol. Lett. 13, 1019–1029. (doi:10.1111/j.1461-0248.2010.01496.x)

37. Capitán JA, Cuenda S, Alonso D. 2017 Stochastic competitive exclusion leads to a cascade of species extinctions. J. Theor. Biol. 419, 137–151. (doi:10.1016/j.jtbi.2017.02.007)

38. Fisher CK, Mehta P. 2014 The transition between the niche and neutral regimes in ecology. Proc. Natl Acad. Sci. USA 111, 13 111–13 116. (doi:10.1073/pnas.1405637111)

39. May R. 1999 Unanswered questions in ecology. Phil. Trans. R. Soc. Lond. B 354, 1951–1959. (doi:10.1098/rstb.1999.0534)

40. Pennisi E. 2005 What determines species diversity? *Science* **309**, 90. (doi:10.1126/science.309.5731.90)

41. Smale S. 1976 On the differential equations of species in competition. *J. Math. Biol.* **3**, 5–7. (doi:10.1007/BF00307854)

42. Moran P. 1962 *The statistical processes of evolutionary theory*. Oxford, UK: Clarendon Press.

43. Lin YT, Kim H, Doering CR. 2012 Features of fast living: on the weak selection for longevity in degenerate birth-death processes. *J. Stat. Phys.* **148**, 646–662. (doi:10.1007/s10955-012-0479-9)

44. Kingman J. 1982 The coalescent. *Stoch. Process. Appl.* **13**, 235–248. (doi:10.1016/0304-4149(82)90011-4)

45. Abrams P. 1983 The theory of limiting similarity. *Annu. Rev. Ecol. Syst.* **14**, 359–376. (doi:10.1146/annurev.es.14.110183.002043)

46. Volterra V. 1926 Fluctuations in the abundance of a species considered mathematically. *Nature* **118**, 558–560. (doi:10.1038/118558a0)

47. Bomze IM. 1983 Lotka-Volterra equation and replicator dynamics: a two-dimensional classification. *Biol. Cybern.* **211**, 201–211. (doi:10.1007/BF00318088)

48. Chesson P. 1990 MacArthur's resource model. *Theor. Popul. Biol.* **37**, 26–38. (doi:10.1016/0040-5809(90)90025-Q)

49. Antal T, Scheuring I. 2006 Fixation of strategies for an evolutionary game in finite populations. *Bull. Math. Biol.* **68**, 1923–1944. (doi:10.1007/s11538-006-9061-4)

50. Kamenev A, Meerson B, Shklovskii B. 2008 How colored environmental noise affects population extinction. *Phys. Rev. Lett.* **101**, 268103. (doi:10.1103/PhysRevLett.101.268103)

51. Chotibut T, Nelson DR, Succi S. 2017 Striated populations in disordered environments with advection. *Phys. A. Stat. Mech. Appl.* **465**, 500–514. (doi:10.1016/j.physa.2016.08.059)

52. Assaf M, Meerson B. 2006 Spectral theory of metastability and extinction in birth-death systems. *Phys. Rev. Lett.* **97**, 1–4. (doi:10.1103/PhysRevLett.97.200602)

53. Gottesman O, Meerson B. 2012 Multiple extinction routes in stochastic population models. *Phys. Rev. E* **85**, 021140. (doi:10.1103/PhysRevE.85.021140)

54. Dobrinevski A, Frey E. 2012 Extinction in neutrally stable stochastic Lotka-Volterra models. *Phys. Rev. E* **85**, 1–14. (doi:10.1103/PhysRevE.85.051903)

55. Gabel A, Meerson B, Redner S. 2013 Survival of the scarcer. *Phys. Rev. E* **87**, 010101. (doi:10.1103/PhysRevE.87.010101)

56. Constable GWA, McKane AJ. 2015 Models of genetic drift as limiting forms of the Lotka-Volterra competition model. *Phys. Rev. Lett.* **114**, 1–5. (doi:10.1103/PhysRevLett.114.038101)

57. Chotibut T, Nelson DR. 2015 Evolutionary dynamics with fluctuating population sizes and strong mutualism. *Phys. Rev. E* **92**, 022718. (doi:10.1103/PhysRevE.92.022718)

58. Young G, Belmonte A. 2018 Explicit probability of fixation formula for mutual competitors in a stochastic population model under competitive trade-offs. (http://arxiv.org/abs/180906917).

59. Norden RH. 1982 On the distribution of the time to extinction in the stochastic logistic population-model. *Adv. Appl. Probab.* **14**, 687–708. (doi:10.2307/1427019)

60. Kamenev A, Meerson B. 2008 Extinction of an infectious disease: a large fluctuation in a non-equilibrium system. *Phys. Rev. E* **77**, 1–4. (doi:10.1103/PhysRevE.77.061107)

61. Assaf M, Meerson B, Sasorov PV. 2010 Large fluctuations in stochastic population dynamics: momentum-space calculations. *J. Stat. Mech: Theory Exp.* **2010**, P07018. (doi:10.1088/1742-5468/2010/07/P07018)

62. Ovaskainen O, Meerson B. 2010 Stochastic models of population extinction. *Trends Ecol. Evol.* **25**, 643–52. (doi:10.1016/j.tree.2010.07.009)

63. Lin YT, Kim H, Doering CR. 2015 Demographic stochasticity and evolution of dispersion I. Spatially homogeneous environments. *J. Math. Biol.* **70**, 647–678. (doi:10.1007/s00285-014-0776-9)

64. Kimura M. 1955 Stochastic processes and distribution of gene frequencies under natural selection. *Cold Spring Harb. Symp. Quant. Biol.* **20**, 33–53. (doi:10.1101/SQB.1955.020.01.006)

65. Chotibut T, Nelson DR. 2017 Population genetics with fluctuating population sizes. *J. Stat. Phys.* **167**, 777–791. (doi:10.1007/s10955-017-1741-y)

66. Wright S. 1931 Evolution in Mendelian populations. *Genetics* **16**, 97.

67. Fisher RA. 1930 *The genetical theory of natural selection*. Oxford, UK: Clare.

68. Rogers J, Gibbs RA. 2014 Comparative primate genomics: emerging patterns of genome content and dynamics. *Nat. Rev. Genet.* **15**, 347–359. (doi:10.1038/nrg3707)

69. Haegeman B, Loreau M. 2011 A mathematical synthesis of niche and neutral theories in community ecology. *J. Theor. Biol.* **269**, 150–165. (doi:10.1016/j.jtbi.2010.10.006)

70. Kessler DA, Shnerb NM. 2015 Generalized model of island biodiversity. *Phys. Rev. E* **91**, 042705. (doi:10.1103/PhysRevE.91.042705)

71. Van Melderen L, De Bast MS. 2009 Bacterial toxin-antitoxin systems: more than selfish entities? *PLoS Genet.* **5**, e1000437. (doi:10.1371/journal.pgen.1000437)

72. Kessler DA, Austin RH, Levine H. 2014 Resistance to chemotherapy: patient variability and cellular heterogeneity. *Cancer Res.* **74**, 4663–4670. (doi:10.1158/0008-5472.CAN-14-0118)

73. Vega NM, Gore J. 2017 Stochastic assembly produces heterogeneous communities in the *Caenorhabditis elegans* intestine. *PLoS Biol.* **15**, 1–20. (doi:10.1371/journal.pbio.2000633)

74. Kessler DA, Shnerb NM. 2007 Extinction rates for fluctuation-induced metastabilities: a real-space WKB approach. *J. Stat. Phys.* **127**, 861–886. (doi:10.1007/s10955-007-9312-2)

75. Leibold MA, McPeek MA. 2006 Coexistence of the niche and neutral perspectives in community ecology. *Ecology* **87**, 1399–1410. (doi:10.1890/0012-9658(2006)87[1399:COTNAN]2.0.CO;2)

76. Ofiţeru ID, Lunn M, Curtis TP, Wells GF, Criddle CS, Francis CA, Sloan WT. 2010 Combined niche and neutral effects in a microbial wastewater treatment community. *Proc. Natl Acad. Sci. USA* **107**, 15 345–15 350. (doi:10.1073/pnas.1000604107)

77. Pigolotti S, Benzi R, Perlekar P, Jensen MH, Toschi F, Nelson DR. 2013 Growth, competition and cooperation in spatial population genetics. *Theor. Popul. Biol.* **84**, 72–86. (doi:10.1016/j.tpb.2012.12.002)

78. Neuhauser C, Pacala SW. 1999 An explicitly spatial version of the Lotka-Volterra model with interspecific competition. *Ann. Appl. Probab.* **9**, 1226–1259. (doi:10.1214/aoap/1029962871)

79. Cox JT, Merle M, Perkins E. 2010 Coexistence in a two-dimensional Lotka-Volterra model. *Electron. J. Probab.* **15**, 1190–1266. (doi:10.1214/EJP.v15-795)

80. Case TJ, Casten R. 1979 Global stability and multiple domains of attraction in ecological systems. *Am. Nat.* **113**, 705–714. (doi:10.1086/283427)

81. Van Kampen NG. 1992 *Stochastic processes in physics and chemistry*. North-Holland, Amsterdam: North Holland.

82. Elgart V, Kamenev A. 2004 Rare event statistics in reaction-diffusion systems. *Phys. Rev. E* **70**, 1–12. (doi:10.1103/PhysRevE.70.041106)

83. Parker M, Kamenev A. 2009 Extinction in the Lotka-Volterra model. *Phys. Rev. E* **80**, 021129. (doi:10.1103/PhysRevE.80.021129)

84. Allen LJS, Allen EJ. 2003 A comparison of three different stochastic population models with regard to persistence time. *Theor. Popul. Biol.* **64**, 439–449. (doi:10.1016/S0040-5809(03)00104-7)

85. Badali M. 2019 Extinction, Fixation, and Invasion in an Ecological Niche. PhD thesis, University of Toronto.

86. Munsky B, Khammash M. 2006 The finite state projection algorithm for the solution of the chemical master equation. *J. Chem. Phys.* **124**, 044104. (doi:10.1063/1.2145882)

87. Grasman J, Ludwig D. 1983 The accuracy of the diffusion approximation to the expected time to extinction for some discrete stochastic processes. *J. Appl. Probab.* **20**, 305–321. (doi:10.2307/3213804)

88. Doering CR, Sargsyan KV, Sander LM. 2005 Extinction times for birth-death processes: exact results, continuum asymptotics, and the failure of the Fokker-Planck approximation. *Multiscale Model. Simul.* **3**, 283–299. (doi:10.1137/030602800)

89. Assaf M, Meerson B. 2017 WKB theory of large deviations in stochastic populations. *J. Phys. A: Math. Theor.* **50**, 263001. (doi:10.1088/1751-8121/aa669a)

90. Parsons TL, Quince C, Plotkin JB. 2010 Some consequences of demographic stochasticity in population genetics. *Genetics* **185**, 1345–1354. (doi:10.1534/genetics.110.115030)

91. Cao Y, Terebus A, Liang J. 2016 State space truncation with quantified errors for accurate solutions to discrete chemical master equation. *Bull. Math. Biol.* **78**, 617–661. (doi:10.1007/s11538-016-0149-1)

92. Hänggi P, Talkner P, Borovec M. 1990 Reaction rate theory: 50 years after Kramers. *Rev. Mod. Phys.* **62**, 251–341. (doi:10.1103/RevModPhys.62.251)

93. Gillespie DT. 1977 Exact stochastic simulation of couple chemical reactions. *J. Phys. Chem.* **81**, 2340–2361. (doi:10.1021/j100540a008)

94. Cao Y, Gillespie DT, Petzold LR. 2006 Efficient step size selection for the tau-leaping simulation method. *J. Chem. Phys.* **124**, 044109. (doi:10.1063/1.2159468)

95. Grinstead CM, Snell LJ. 2003 *Introduction to probability*, 2nd edn. Providence, RI: American Mathematical Society.

96. Iyer-Biswas S, Zilman A. 2016 First passage processes in cellular biology. *Adv. Chem. Phys.* **16**, 261–306.

97. Guennebaud G, Jacob B, Avery P, Bachrach A, Barthelemy S. 2010 Eigen v3. http://eigen.tuxfamily.org.

98. Lambert A. 2005 The branching process with logistic growth. *Ann. Appl. Probab.* **15**, 1506–1535. (doi:10.1214/105051605000000098)

99. Lande R. 1993 Risks of population extinction from demographic and environmental stochasticity and random catastrophes. *Am. Nat.* **142**, 911–927. (doi:10.1086/285580)

100. Roozen H. 1987 Equilibrium and extinction in stochastic population dynamics. *Bull. Math. Biol.* **49**, 671–696. (doi:10.1016/S0092-8240(87)90014-0)

101. Roozen H. 1989 An asymptotic solution to a two-dimensional exit problem arising in population dynamics. *SIAM J. Appl. Math.* **49**, 1793–1810. (doi:10.1137/0149110)

102. Matkowsky B, Schuss Z, Knessl C, Tier C, Mangel M. 1984 Asymptotic solution of the Kramers-Moyal equation and first-passage times for Markov jump processes. *Phys. Rev. A* **29**, 3359. (doi:10.1103/PhysRevA.29.3359)

103. Zhou JX, Aliyu MDS, Aurell E, Huang S. 2012 Quasi-potential landscape in complex multi-stable systems. *J. R. Soc. Interface* **9**, 3539–3553. (doi:10.1098/rsif.2012.0434)

104. Berglund N. 2013 Kramers' law: validity, derivations and generalisations. *Markov Processes and Related Fields* **19**, 459–490.

105. Nisbet RM, Gurney WSC. 1982 *Modelling fluctuating populations*. Toronto, Canada: John Wiley & Sons.

106. Grasman J. 1996 The expected extinction time of a population within a system of interacting biological populations. *Bull. Math. Biol.* **58**, 555–568. (doi:10.1007/BF02460596)

107. Kimura M. 1964 Diffusion models in population genetics. *J. Appl. Probab.* **1**, 177–232. (doi:10.2307/3211856)

108. Dias PC. 1996 Sources and sinks in population biology. *Trends Ecol. Evol.* **11**, 326–330. (doi:10.1016/0169-5347(96)10037-9)

109. Mangel M, Ludwig D. 1977 Probability of extinction in a stochastic competition. *SIAM J. Appl. Math.* **33**, 256–266. (doi:10.1137/0133015)

110. McKane AJ, Tarlie MB. 2004 Optimal paths and the calculation of state selection probabilities. *Phys. Rev. E* **69**, 041106. (doi:10.1103/PhysRevE.69.041106)

111. Lambert A. 2006 Probability of fixation under weak selection: a branching process unifying approach. *Theor. Popul. Biol.* **69**, 419–441. (doi:10.1016/j.tpb.2006.01.002)

112. Czuppon P, Traulsen A. 2018 Fixation probabilities in populations under demographic fluctuations. *J. Math. Biol.* **77**, 1233–1277. (doi:10.1007/s00285-018-1251-9)

113. Parsons TL. 2018 Invasion probabilities, hitting times, and some fluctuation theory for the stochastic logistic process. *J. Math. Biol.* **77**, 1193–1231. (doi:10.1007/s00285-018-1250-x)

114. MacArthur RH. 1957 On the relative abundance of bird species. *Proc. Natl Acad. Sci. USA* **43**, 293–295. (doi:10.1073/pnas.43.3.293)

115. Shmida A, Ellner S. 1984 Coexistence of plant-species with similar niches. *Vegetatio* **58**, 29–55.

116. Bez W, Talkner P. 1981 A new variational method to calculate escape rates in bistable systems. *Phys. Lett. A* **82**, 313–316. (doi:10.1016/0375-9601(81)90903-8)

117. Hung PJ, Lee PJ, Sabounchi P, Aghdam N, Lin R, Lee LP. 2005 A novel high aspect ratio microfluidic design to provide a stable and uniform microenvironment for cell growth in a high throughput mammalian cell culture array. *Lab Chip* **5**, 44–8. (doi:10.1039/b410743h)

118. Chesson PL, Huntly N. 1997 The roles of harsh and fluctuating conditions in the dynamics of ecological communities. *Am. Nat.* **150**, 519–553. (doi:10.1086/286080)

119. Frey E. 2010 Evolutionary game theory: theoretical concepts and applications to microbial communities. *Physica A* **389**, 4265–4298. (doi:10.1016/j.physa.2010.02.047)

120. Badali M, Zilman A. 2020 Data from: Effects of niche overlap on coexistence, fixation and invasion in a population of two interacting species. Dryad Digital Repository. (doi:10.5061/dryad.t76hdr7xg)